Analytic Equation of State for Lennard-Jones Fluids Based on the Ross Variational Perturbation Theory

Jiuxun Sun,[1,2] **LingCang Cai,**[3] **Qiang Wu,**[3] **and Fuqian Jing**[3]

By using a previously developed analytic expression for the radial distribution function of hard spheres, a simple analytic equation of state (EOS) for fluids with a continuous Lennard-Jones potential is established based on Ross's variational perturbation theory. The main thermodynamic quantities have been analytically derived, the resulting expressions are surprisingly simple, the variational procedure is greatly simplified, and the calculations are absolutely convergent. The numerical results are compared with the Monte-Carlo data and the original Ross variational theory. It is shown that the precision of the analytic EOS is as good as the original non-analytic one, and their applicable range is believed identical. A comparison with the recently proposed mean-sphere-approximation theory shows that the analytic equation of state developed here has wider applicability and precision.

KEY WORDS: analyticity; equation of state; statistical mechanics; variational perturbation theory.

1. INTRODUCTION

Perturbation theories such as the Barker–Henderson (BH) [1], the Weeks–Chandler–Anderson (WCA) [2] theories and the Ross theory [3] are most frequently used in research on the thermodynamic properties of fluids both at normal conditions and at conditions with high temperature and high density. The perturbation theories require knowledge of the equation of

---

[1] Department of Applied Physics, University of Electronic Science and Technology, Chengdu 610054, People's Republic of China.
[2] To whom correspondence should be mailed. E-mail: sjx@uestc.edu.cn
[3] Laboratory for Shock Wave and Detonation Physics Research, Southwest Institute of Fluid Physics, P.O. Box 919-102, Mianyang 621900, People's Republic of China.

state (EOS) and the radial distribution function (r.d.f.) of a reference hard-sphere fluid. For this fluid, the Carnahan–Starling (CS) EOS [4] combines simplicity and accuracy. As for the r.d.f., there are available analytical expressions for the r.d.f. from the solution of the Percus–Yevick (PY) integral equation [5, 6]. However, although the Laplace transformation of the PY r.d.f. is simple enough, its expression in coordinate space is too complicated to be convenient for practical applications. This results in the perturbation schemes having manifestly failed to provide a generally analytic and applicable EOS even for the simplest square-well or Sutherland fluids. Theories developed subsequently prefer the numerical table given by Troop and Bearman rather than the analytic PY expression [7], such as the mode expansion theory for electrolyte solutions [8] and renormalization theory for simple fluids [9]. Moreover, it is known that the PY solution is not sufficiently accurate, particularly for radial distances close to contact. Therefore, a considerable number of procedures have been developed to improve the r.d.f. obtained from integral equation theories [10–14]. In most cases, the resulting r.d.f. becomes more complicated than the PY expression or even nonanalytical, which makes its use impractical, particularly in the context of perturbation theories.

    In Ref. 15, Largo and Solana developed a semi-empirical analytic expression for the r.d.f. of hard spheres, and they have developed an analytic equation of state (EOS) for the square-well [15] and Sutherland fluids [16] based on the BH perturbation theory. However, they have not carefully selected the form of their expression for the r.d.f. of hard spheres; the developed expression has not used any information from the CS EOS, so it cannot reproduce the CS EOS, and the expression is too complicated with only moderate precision. It contains 128 terms, which seems excessive, and the resulting EOS even for the simplest Sutherland fluid contains at least 250 terms.

    Very recently, we developed an alternative analytic expression for the r.d.f. of hard spheres [17]. The expression has successfully overcome the shortcomings of Largo and Solana's expression, and combined the simplicity, accuracy and analyticity in it. In the same work, we have developed an analytic EOS for Sutherland fluids; the EOS only contains about twenty terms, and its simplicity is superior to the one developed by Largo and Solana [16]. Here, we further develop an analytic EOS for Lennard-Jones fluids. Since in BH and WCA perturbation theories, the numerical results are very sensitive to the effective diameter of the reference fluid [16], we would use the Ross variational theory [3] for which the effective diameter is well defined and is chosen as that value minimizing the Helmholtz free energy.

    The Ross variational theory is one of the most accurate perturbation theories. It has been widely used in research on shock-compressed properties

of materials [18, 19]. Its main disadvantage lies in the variational procedure being too time-consuming and very inconvenient. In order to overcome these shortcomings, Tang et al. have alternatively developed a mean-sphere-approximation (MSA) theory [20–22]. However, the MSA theory also has some disadvantages that are more severe than the Ross theory. The most important is that the MSA theory is inapplicable to fluids at high temperature and density, and at other conditions, the theory only gives results comparable with the Ross theory or even poorer. If the Ross theory can provide an analytic EOS, it may have advantages compared to other perturbation approaches. Although it may seem unimaginable to develop an analytic EOS based on a variational theory [20–22], we can see that the resulting analytic EOS developed in this paper is surprisingly simple and the precision almost has not been lost. In Section 2, the analytic EOS is developed, and in Section 3 the numerical results are presented and discussed.

2. DEVELOPMENT OF ANALYTIC EQUATION OF STATE

In terms of the Ross perturbation theory [3], the excess Helmholtz free energy can be expressed as follows:

$$\frac{F}{NkT} = \frac{F_0}{NkT} + \frac{F_1}{NkT} + \frac{F_{12}(\eta)}{NkT} \tag{1}$$

where F_0 is the excess free energy of the reference hard-sphere system, and is usually obtained by CS EOS [3, 4], and

$$\frac{F_1}{NkT} = 2\pi\rho\beta \int_d^\infty \phi(r)\, g(r)\, r^2\, dr \tag{2}$$

is the first-order perturbation. $F_{12}(\eta)$ is a function making Eq. (1) reproduce the Monte-Carlo inverse 12th-power results [3]. It is dependent on the form of the r.d.f of hard spheres. By using the analytic expression for $g(r)$ developed in Ref. 17, the determined $F_{12}(\eta)$ is slightly different from Ross's [3] and is given by

$$\frac{F_{12}(\eta)}{NkT} = -(\eta/2 + 15\eta^3/4) \tag{3}$$

where $\eta = \pi\rho d^3/6$, and η is employed as the variational parameter that minimizes the right-hand side of Eq. (1). Namely, η should be determined by

$$\frac{\partial}{\partial\eta}\left(\frac{F}{NkT}\right)_{T,\rho} = 0 \tag{4}$$

Table I. Coefficients Contained in the Analytic Expression of Radial Distribution Function of Hard Spheres in Eqs. (5) and (6)

	m	n			
		0	1	2	3
A_{mn}	1	2.5	−0.2975	−1.4243	0.4141
	2	2	−4.0464	−2.1422	2.0767
	3	0.5	−6.3781	10.13	−3.6507
B_{mn}	1	−0.34	−0.3317	0.5555	−0.1402
	2	1	2.8897	−3.1078	0.6822
	3	−0.29	−2.619	2.1554	−0.3989

The analytic expression of $g(r)$ developed in Ref. 17 is as follows

$$g(x) = \begin{cases} 0, & (x < 1) \\ 1 + \sum_{m=1}^{3} \dfrac{\eta^m}{(1-\eta)^m} g_m(x), & (1 \leqslant x < 3) \\ 1, & (x \geqslant 3) \end{cases} \quad (5)$$

In Eq. (5), x is the radial coordinate reduced by the hard sphere diameter d, and

$$g_m(x) = \begin{cases} \sum_{n=0}^{3} A_{mn}(x - x^{-4})^n, & (1 \leqslant x < 2), \\ \sum_{n=0}^{3} B_{mn}(x - 256x^{-7})^n, & (2 \leqslant x < 3). \end{cases} \quad (6)$$

The coefficients A_{mn} and B_{mn} have been listed in Table I.

The LJ potential has the form

$$\phi(r) = 4\varepsilon \left[\left(\frac{\sigma}{r} \right)^{12} - \left(\frac{\sigma}{r} \right)^{6} \right] \quad (7)$$

Substituting Eqs. (5) and (7) into Eq. (2), and introducing the variable transformation $r = dx$, we obtain

$$\frac{F_1}{NkT} = 8\pi\rho \, d^3\beta \, \varepsilon \int_d^\infty \left[\left(\frac{\sigma}{d} \right)^{12} \frac{1}{x^{12}} - \left(\frac{\sigma}{d} \right)^{6} \frac{1}{x^{6}} \right] g(x) \, x^2 \, dx$$

$$= 8\pi\rho \, d^3\beta \, \varepsilon \int_d^\infty \left[\left(\frac{\eta_e}{\eta} \right)^{4} \frac{1}{x^{12}} - \left(\frac{\eta_e}{\eta} \right)^{2} \frac{1}{x^{6}} \right] \left[1 + \sum_{m=1}^{3} \frac{\eta^m}{(1-\eta)^m} g_m(x) \right] x^2 \, dx$$

or

$$\frac{F_1}{NkT} = 48\eta\beta\varepsilon \sum_{m=0}^{3} \frac{\eta^m}{(1-\eta)^m} \left[\left(\frac{\eta_e}{\eta}\right)^4 Q_{rm} - \left(\frac{\eta_e}{\eta}\right)^2 Q_{am} \right] \tag{8}$$

where $\eta_e = \pi\rho\sigma^3/6$ is the reduced density. Q_{rm} and Q_{am} are auxiliary constants defined by

$$\begin{cases} Q_{r0} = \int_1^\infty \frac{1}{x^{10}} \, dx = \frac{1}{9} \\ Q_{a0} = \int_1^\infty \frac{1}{x^4} \, dx = \frac{1}{3} \end{cases} \tag{9a}$$

and

$$\begin{cases} Q_{rm} = \int_1^\infty \frac{1}{x^{10}} g_m(x) \, dx = \int_1^2 \frac{1}{x^{10}} g_m(x) \, dx + \int_2^3 \frac{1}{x^{10}} g_m(x) \, dx \\ Q_{am} = \int_1^\infty \frac{1}{x^4} g_m(x) \, dx = \int_1^2 \frac{1}{x^4} g_m(x) \, dx + \int_2^3 \frac{1}{x^4} g_m(x) \, dx \end{cases} \tag{9b}$$

The values have been evaluated and listed in Table II.

Substituting Eqs. (3) and (8) into Eq. (1), and Eq. (1) into Eq. (4), the equation to determine η can be derived as

$$\frac{4-2\eta}{(1-\eta)^3} - \frac{1}{2} - \frac{45}{4}\eta^2 + 48\beta\varepsilon \sum_{m=0}^{3} C_m \frac{\eta^m}{(1-\eta)^{m+1}} = 0 \tag{10}$$

and

$$C_m = \left(\frac{\eta_e}{\eta}\right)^4 (m-3+3\eta) \, Q_{rm} - \left(\frac{\eta_e}{\eta}\right)^2 (m-1+\eta) \, Q_{am} \tag{11}$$

Table II.   Values of Coefficients Defined in Eq. (9)

m	Q_{rm}	Q_{am}
0	1/9	1/3
1	0.227675	0.425596
2	0.021796	−0.190918
3	−0.018935	0.047583

Although Eq. (10) is a nonlinear algebraic equation, by using the Newton iteration approach, its solution is insensitive to the initial value and is absolutely convergent.

The compressibility factor can be derived as follows,

$$\frac{PV}{NkT} = 1 + \rho \frac{\partial}{\partial \rho} \left(\frac{F}{NkT} \right)_T = 1 + \eta_e \frac{\partial}{\partial \eta_e} \left(\frac{F}{NkT} \right)_T$$

$$= 1 + \eta_e \frac{\partial}{\partial \eta_e} \left(\frac{F}{NkT} \right)_{T,\eta} + \frac{\partial}{\partial \eta} \left(\frac{F}{NkT} \right)_{T,\eta_e} \cdot \eta_e \frac{\partial \eta}{\partial \eta_e}$$

Considering Eq. (4), the third term in the equation equals zero, and we obtain

$$\frac{PV}{NkT} = 1 + \eta_e \frac{\partial}{\partial \eta_e} \left(\frac{F}{NkT} \right)_{T,\eta} = 1 + \eta_e \frac{\partial}{\partial \eta_e} \left(\frac{F_1}{NkT} \right)_{T,\eta}$$

$$= 1 + 48\eta\beta\varepsilon \sum_{m=0}^{3} \frac{\eta^m}{(1-\eta)^m} \left[\left(\frac{\eta_e}{\eta} \right)^4 4Q_{rm} - \left(\frac{\eta_e}{\eta} \right)^2 2Q_{am} \right] \quad (12)$$

The equation to evaluate the excess internal energy of the system is

$$\frac{U}{NkT} = \beta \frac{\partial}{\partial \beta} \left(\frac{F}{NkT} \right)_\rho = \beta \frac{\partial}{\partial \beta} \left(\frac{F}{NkT} \right)_\eta + \frac{\partial}{\partial \eta} \left(\frac{F}{NkT} \right)_{T,\eta_e} \beta \frac{\partial \eta}{\partial \beta}$$

Considering Eq. (4), the second term in the equation also equals zero, and the equation is changed to

$$\frac{U}{NkT} = \beta \frac{\partial}{\partial \beta} \left(\frac{F}{NkT} \right)_\eta = \beta \frac{\partial}{\partial \beta} \left(\frac{F_1}{NkT} \right)_\eta = \frac{F_1}{NkT} \quad (13)$$

By using these equations, all other thermodynamic quantities can be evaluated analytically. For example, the excess entropy of the system is

$$\frac{S}{Nk} = \frac{U}{NkT} - \frac{F}{NkT} = -\frac{F_0}{NkT} - \frac{F_{12}(\eta)}{NkT} \quad (14)$$

and the excess Gibbs free enthalpy is

$$\frac{G}{NkT} = \frac{F}{NkT} + \frac{PV}{NkT} - 1 = \frac{F_0}{NkT} + \frac{F_{12}(\eta)}{NkT}$$

$$+ 48\eta\beta\varepsilon \sum_{m=0}^{3} \frac{\eta^m}{(1-\eta)^m} \left[\left(\frac{\eta_e}{\eta} \right)^4 5Q_{rm} - \left(\frac{\eta_e}{\eta} \right)^2 3Q_{am} \right] \quad (15)$$

Now we determine the second virial coefficient. The virial expansion is as follows

$$\frac{PV}{NkT} = 1 + B_r \frac{2}{3} \pi \rho \sigma^3 + C_r \left(\frac{2}{3} \pi \rho \sigma^3 \right)^2 + \cdots$$

$$= 1 + B_r(4\eta_e) + C_r(4\eta_e)^2 + \cdots$$

B_r is the second virial coefficient divided by $2\sigma^3/3$; it can be determined by the equation

$$B_r = \frac{1}{4} \lim_{\eta_e \to 0} \frac{1}{\eta_e} \left(\frac{PV}{NkT} - 1 \right) \tag{16}$$

Substituting Eq. (12) into Eq. (16), we obtain

$$B_r = 24\gamma_0 \beta \varepsilon (2Q_{r0}\gamma_0^2 - Q_{a0}) \tag{17}$$

where

$$\gamma_0 = \lim_{\eta_e \to 0} (\eta_e/\eta) \tag{18}$$

Its value can be calculated from Eqs. (10) and (11).

3. NUMERICAL RESULTS AND DISCUSSION

From the expressions derived in the previous section, we have calculated the compressibility factor, excess internal energy, and the configurational free energy. In Table III, the results are compared with the Monte-Carlo (MC) data [3, 23] and Ross' numerical results [3]. The table shows that the agreement of our results with the MC data for some density and temperature points is better than that of the Ross results, and in some points is slightly poorer, but the overall agreement is almost identical. Table IV further gives the comparison of our results and Ross' results with MC data [3, 23] in the critical region. It is shown that the present analytic theory compares favorably with these results, except near the critical point.

In Fig. 1, the calculated pressure and internal energy for three typical temperatures are also compared with the MC data and the results from the MSA theory [20]. It is shown that our results are almost completely in agreement with the MC data points, but the MSA results have obvious deviations from the MC data, and the deviations become larger for higher temperature and density. For the temperature $kT/\varepsilon = 5$, the largest relative error for the density considered is at least 10%, and for $kT/\varepsilon = 100$,

Table III. Comparison of Lennard-Jones Thermodynamic Properties from Monte-Carlo (MC), from Original Perturbation Theory of Ross (R), and from Present Theory (S) at High Temperature and Density. ($PV/(NkT)$) is the compressibility factor, U is the excess internal energy, and F is the excess configurational free energy.)

kT/ε	$\rho\sigma^3$	$PV/(NkT)$			$U/(NkT)$			$F/(NkT)$		
		MC	R	S	MC	R	S	MC	R	S
100	0.2	1.22	1.22	1.22	0.036	0.034	0.034	0.21	0.20	0.20
	0.4	1.51	1.50	1.51	0.085	0.081	0.083	0.45	0.44	0.44
	0.5	1.68	1.67	1.68	0.115	0.111	0.114	0.58	0.56	0.57
	0.666	2.00	2.01	2.02	0.175	0.173	0.176	0.82	0.80	0.81
	1	2.95	2.96	2.96	0.361	0.376	0.358	1.39	1.38	1.39
	1.333	4.36	4.40	4.38	0.648	0.652	0.647	2.13	2.13	2.14
	1.4	4.76	4.76	4.74	0.734	0.729	0.722	2.31	2.30	2.31
	2	9.50	9.56	9.55	1.767	1.779	1.774	4.36	4.36	4.36
	2.222	12.10	12.26	12.29	2.346	2.385	2.391	5.38	5.39	5.39
	2.38	14.46	14.56	14.64	2.887	2.909	2.929	6.22	6.25	6.25
	2.5	16.29	16.54	16.69	3.304	3.356	3.398	6.92	5.95	5.96
20	0.2	1.27	1.26	1.26	−0.005	−0.010	−0.008		0.23	0.24
	0.4	1.67	1.65	1.67	0.009	0.001	0.004		0.53	0.53
	0.5	1.93	1.92	1.93	0.026	0.018	0.021		0.69	0.71
	0.666	2.51	2.51	2.52	0.083	0.074	0.075		1.03	1.05
	1	4.46	4.49	4.45	0.348	0.343	0.334		1.98	2.00
	1.333	8.00	8.09	8.06	0.942	0.958	0.948		3.43	3.43
	1.765	16.68	16.75	16.93	2.65	2.65	2.69		6.45	6.46
5	0.2	1.17	1.15	1.16	−0.202	−0.200	−0.198		0.12	0.12
	0.5	1.82	1.82	1.82	−0.474	−0.488	−0.487		0.45	0.47
	0.666	2.67	2.67	2.65	−0.584	−0.592	−0.598		0.80	0.81
	1	6.34	6.49	6.45	−0.456	−0.448	−0.461		2.08	2.08
	1.279	13.44	13.46	13.59	0.435	0.413	−0.432		4.16	4.16
2.74	0.2	0.99	0.96	0.97	−0.440	−0.410	−0.408	−0.04	−0.06	−0.05
	0.4	1.20	1.14	1.15	−0.865	−0.855	−0.853	−0.01	−0.05	−0.03
	0.7	2.59	2.57	2.51	−1.424	−1.454	−1.468	0.38	0.30	0.30
	0.8	3.61	3.65	3.58	−1.562	−1.577	−1.594	0.65	0.57	0.57
	0.9	5.14	5.21	5.16	−1.609	−1.622	−1.638	1.05	0.97	0.96
	1	7.37	7.37	7.38	−1.525	−1.559	−1.567	1.58	1.52	1.51
	1.1	10.17	10.30	10.39	−1.351	−1.352	−1.348	2.31	2.26	2.25

it reaches 30%. It has been shown that the analytic Ross theory is fast and easy for calculations, and the precision is superior to the recently developed MSA theory.

In the non-analytic Ross theory, it is difficult to calculate the second virial coefficient and vapor-liquid equilibrium (VLE). However, based on our analytic EOS, it is simple to make such calculations. In Fig. 2, we show the comparison for the second virial coefficient calculated from our EOS, BH theory [1], and exact results. It can be shown that the results from BH
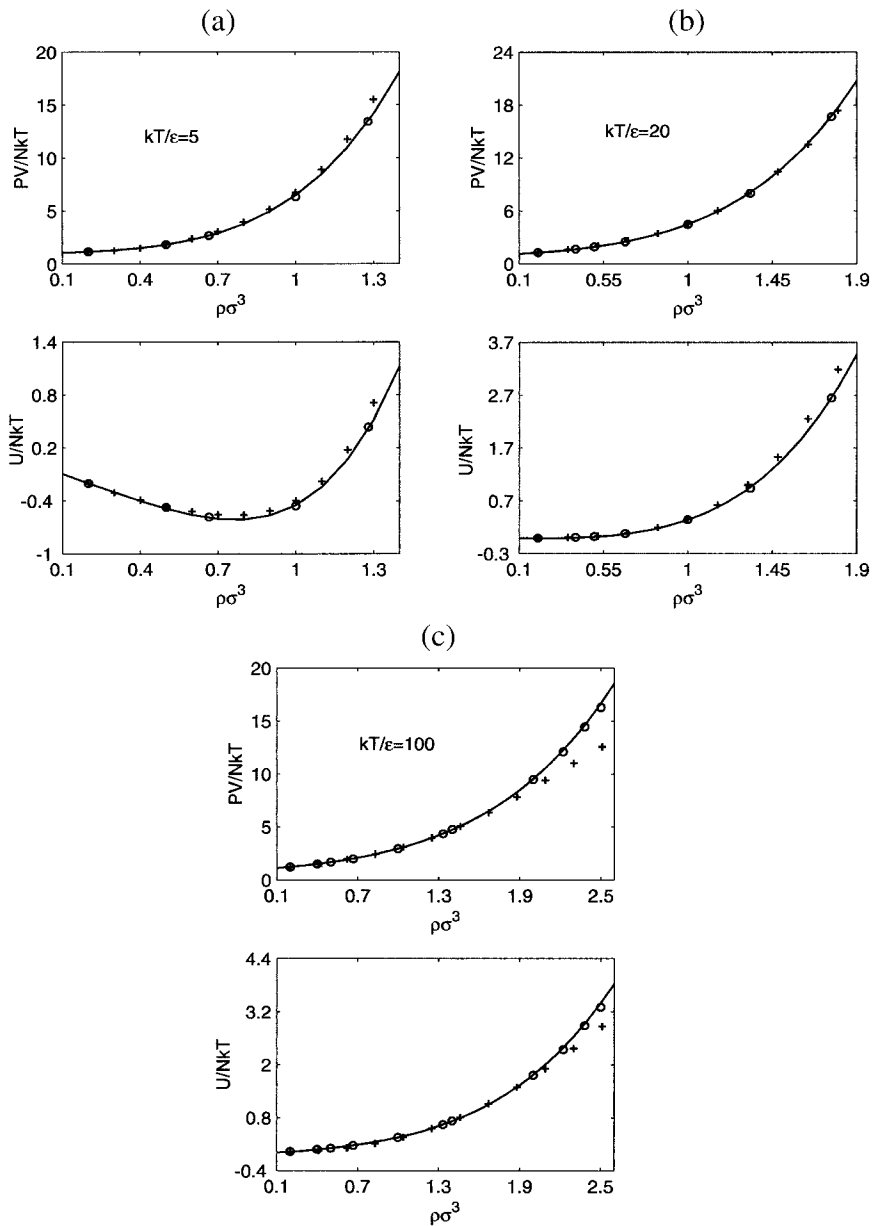
Fig. 1. Comparison of thermodynamic properties for Lennard-Jones fluids versus reduced density ($\rho\sigma^3$) from Monte-Carlo (circles), from mean-sphere-approximation (MSA) theory (crosses), and present theory (solid lines). $PV/(NkT)$ is the compressibility factor, $U/(NkT)$ is the excess internal energy. (a) $kT/\varepsilon = 5$, (b) $kT/\varepsilon = 20$, (c) $kT/\varepsilon = 100$.

theory are in better agreement with the exact results than our results at low temperature, but the BH theory diverges at high temperature, and our EOS gives very good results at high temperature. Considering that the contribution of the second virial expansion to thermodynamic properties at low density is small, our results for the second virial coefficient can be seen as having acceptable precision overall. By using the formula developed in Section 2, we also made the VLE calculations. The determined reduced critical temperature, density, and pressure are given by

$$kT_c/\varepsilon = 1.497, \qquad \rho_c\sigma^3 = 0.326, \qquad P_c\sigma^3/\varepsilon = 0.1896 \qquad (19)$$

and the calculated saturated vapor pressure, saturated liquid density, and saturated vapor density can be well fitted by the following equations:

$$\ln(P_s\sigma^3/\varepsilon) = B_1 + B_2(\varepsilon/kT) + B_3 \ln(kT/\varepsilon) \qquad (20)$$

$$\rho_l\sigma^3 = \rho_c\sigma^3 + B_1\tau + (B_2 + B_3\tau^{1/2})\,\tau^{0.324} \qquad (21)$$

$$\rho_g\sigma^3 = \rho_c\sigma^3 + B_1\tau + (B_2 + B_3\tau^{1/2})\,\tau^{0.324} \qquad (22)$$

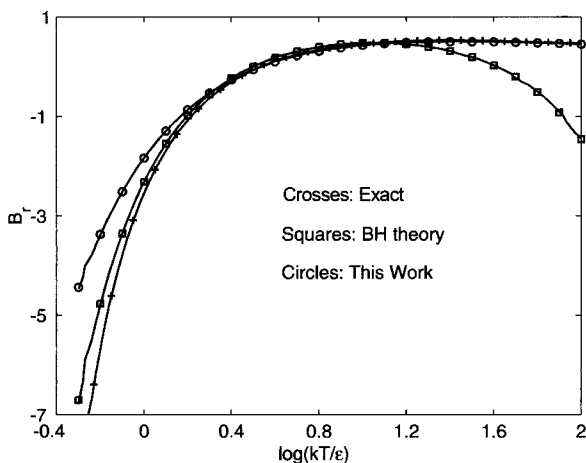The coefficients contained in these equations and the fitting error are listed in Table V.

Fig. 2. Comparison of reduced second virial coefficients (B_r) for Lennard-Jones fluids versus reduced temperature (kT/ε) from exact calculations (crosses), Barker–Henderson (BH) perturbation theory (squares), and present theory (circles).

Table IV. Same as for Table III, but at Critical Region

kT/ε	$\rho\sigma^3$	PV/(NkT)			U/(NkT)			F/(NkT)		
		MC	R	S	MC	R	S	MC	R	S
2.74	0.65	2.22	2.17	2.12		−1.37	−1.38		0.20	0.21
	0.75	3.05	3.06	2.99		−1.52	−1.54		0.42	0.42
	0.85	4.38	4.36	4.30		−1.61	−1.63		0.75	0.75
	0.95	6.15	6.20	6.18		−1.61	−1.62		1.22	1.21
1.35	0.10	0.72	0.75	0.75	−0.58	−0.42	−0.42	−0.29	−0.25	−0.24
	0.20	0.50	0.50	0.51		−0.88	−0.88		−0.50	−0.49
	0.30	0.35	0.27	0.28	−1.55	−1.38	−1.37	−0.80	−0.75	−0.73
	0.40	0.27	0.12	0.12		−1.90	−1.89		−0.98	−0.96
	0.50	0.30	0.14	0.11	−2.50	−2.43	−2.44	−1.16	−1.18	−1.17
	0.55	0.41	0.23	0.19		−2.70	−2.71		−1.26	−1.25
	0.65	0.80	0.70	0.63		−3.23	−3.24		−1.35	−1.35
	0.75	1.73	1.68	1.60		−3.70	−3.72		−1.33	−1.35
	0.85	3.37	3.39	3.36		−4.01	−4.10		−1.15	−1.17
	0.90	4.58	4.60	4.60	−4.19	−4.22	−4.24	−0.91	−0.98	−1.00
	0.95	6.32	6.08	6.12	−4.23	−4.31	−4.33	−0.67	−0.75	−0.77
1.00	0.75	0.58	0.45	0.37		−5.23	−5.26		−2.66	−2.68
	0.85	2.27	2.33	2.31		−5.84	−5.87		−2.63	−2.65
	0.95	3.50	3.73	3.74		−6.25	−6.29		−2.32	−2.35
0.81	0.801	0.06	0.07	0.03	−7.07	−7.08	−7.10		−4.00	−4.03
	0.8839	1.95	226	2.21	−7.71	−7.68	−7.72		−3.99	−4.03
0.75	0.70	−1.71	−1.87	−1.98	−6.76	−6.72	−6.75	−4.17	−4.26	−4.28
	0.80	−0.53	−0.48	−0.53	−7.71	−7.70	−7.74	−4.47	−4.56	−4.60
	0.84	0.37	0.42	0.42	−8.05	−8.06	−8.09	−4.53	−4.62	−4.65
0.72	0.835	−0.08	0.02	−0.01	−8.40	−8.39	−8.43		−4.95	−4.98
	0.85	0.40	0.43	0.40		−8.52	−8.56		−4.96	−5.00
	0.9158	2.25	2.69	2.61	−9.08	−9.03	−9.09		−4.93	−4.97

Table V. Coefficients Contained in Fitting Expressions in Eqs. (20) and (22)

Eqs.	B_1	B_2	B_3	$\Delta\%$
(20)	3.144	−6.972	−0.371	0.30
(21)	−0.1891	0.2883	0.6526	0.33
(22)	1.6508	−0.2291	−1.7088	4.60

The MC simulation data of VLE for the LJ fluid have been given in Refs. 24 and 25. The data for the critical point are

$$kT_c/\varepsilon = 1.309, \qquad \rho_c\sigma^3 = 0.307, \qquad P_c\sigma^3/\varepsilon = 0.1303$$

By comparing these quantities with Eqs. (19), we find the agreement between these equations is not good. In Fig. 3, we compared the saturated vapor pressure given by Eq. (20) with the MC data [23, 24]. It is shown that the agreement is very good. The VLE properties from Eqs. (21) and (22) have been compared with the MC data [24, 25] in Fig. 4. The figure shows the difference is fairly large, especially near the critical point. We think the tendency is in accordance with Table III. Since Tables II and III show that the thermodynamic properties from our EOS are in good agreement with the non-analytic Ross theory, we may impute the inaccuracy near and at the critical point not to the procedure for the establishment of our EOS, but to the Ross theory itself. Thus the range of validity of the EOS in Eq. (12) should eliminate the critical range as did the original Ross theory.

In summary, we have shown that, by using the analytic expression for the radial distribution function of hard spheres previously developed, it is possible to establish a simple analytic EOS for fluids with the continuous Lennard-Jones potential based on a variational perturbation theory. The precision of the analytic EOS is as good as the original non-analytic one. The main thermodynamic quantities can be analytically derived, the obtained expressions are surprisingly simple, and the variational calculations are absolutely convergent. The applicable range of the analytic theory
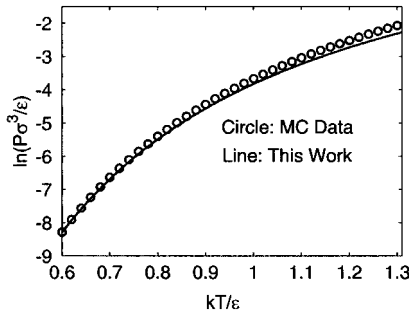

Fig. 3. Comparison of reduced saturated vapor pressure $(\ln(P\sigma^3/\varepsilon))$ for Lennard-Jones fluids versus reduced temperature (kT/ε) from MC data (circles), and present theory (line).
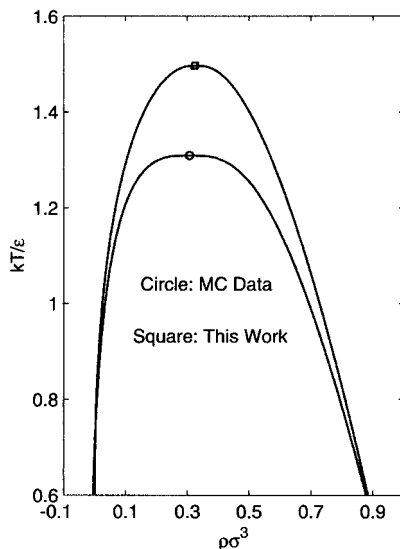
Fig. 4. Orthobaric reduced saturated-vapor and -liquid densities ($\rho\sigma^3$) for Lennard-Jones fluids. Symbols: critical points. Line with circle: MC simulation results. Line with square: this work.

is as same as the original one. It is interesting and practically meaningful to extend the procedure to other perturbation theories or potential systems.

ACKNOWLEDGMENTS

REFERENCES

1. J. A. Barker and D. Henderson, *J. Chem. Phys.* **47**:4714 (1967).
2. J. D. Weeks, D. Chandler, and H. C. Andersen, *J. Chem. Phys.* **54**:5237 (1971).
3. M. Ross, *J. Chem. Phys.* **71**:1567 (1979).
4. N. F. Carnahan and K. E. Starling, *J. Chem. Phys.* **51**:635 (1969).
5. M. S. Wertheim, *Phys. Rev. Lett.* **10**:321 (1963).
6. E. Thiele, *J. Chem. Phys.* **39**:474 (1963).
7. G. J. Troop and R. J. Bearman, *J. Chem. Phys.* **42**:2408 (1965).
8. H. C. Anderson and D. Chandler, *J. Chem. Phys.* **55**:1497 (1971).

9. J. A. White, *J. Chem. Phys.* **113**:1580 (2000).
10. W. R. Smith and D. Henderson, *Molec. Phys.* **19**:411 (1970).
11. J. Chang and S. I. Sandler, *Molec. Phys.* **81**:735 (1994).
12. S. Bravo Yuste and A. Santos, *Phys. Rev. A* **43**:5418 (1991).
13. S. Bravo Yuste, M. López de Haro, and A. Santos, *Phys. Rev. E* **53**:4820 (1996).
14. Y. Tang and B. C.-Y. Lu, *J. Chem. Phys.* **100**:6665 (1994).
15. J. Largo and J. R. Solana, *Fluid Phase Equil.* **167**:21 (2000).
16. J. Largo and J. R. Solana, *Int. J. Thermophys.* **21**:899 (2000).
17. S. Jiuxun, *Simple Analytic Expression for the Radial Distribution Function of Hard Spheres*, *Chinese Phys. Lett.*, to appear.
18. M. Ross, F. H. Ree, and D. A. Young, *J. Chem. Phys.* **79**:487 (1983).
19. N. C. Holmcs, M. Ross, and W. L. Ncllis, *Phys. Rev. B* **52**:15835 (1995).
20. Y. Tang, *J. Chem. Phys.* **116**:6694 (2002).
21. Y. Tang and B. C.-Y. Lu, *Fluid Phase Equilib.* **171**:27 (2000).
22. Y. Tang, Z. Wang, and B. C.-Y. Lu, *Mol. Phys.* **99**:65 (2001).
23. H. S. Kang, C. S. Lee, T. Ree, and F. H. Ree, *J. Chem. Phys.* **82**:414 (1985).
24. A. Trokhymchuk and J. Alejandre, *J. Chem. Phys.* **111**:8510 (1999).
25. D. J. Adams, *Mol. Phys.* **32**:647 (1976).